Dynamics of triplet migration in films of *N*, *N*'-diphenyl-*N*, *N*'-bis(1-naphthyl)-1, 1'-biphenyl-4, 4''-diamine

2010 J. Phys.: Condens. Matter 22 185802

(http://iopscience.iop.org/0953-8984/22/18/185802)

J. Phys.: Condens. Matter **22** (2010) 185802 (11pp) doi:10.1088/0953-8984/22/18/185802

Dynamics of triplet migration in films of N,N'-diphenyl-N,N'-bis(1-naphthyl)-1,1′-biphenyl-4,4″-diamine

Vygintas Jankus[1,3], Chris Winscom[2] and Andrew P Monkman[1]

[1] OEM Research Group, Department of Physics, University of Durham, Durham DH1 3LE, UK
[2] Centre for Phosphors and Display Materials, Wolfson Centre for Materials Processing, Brunel University, Uxbridge, Middlesex UB8 3PH, UK

E-mail: vygintas.jankus@durham.ac.uk

Received 8 January 2010, in final form 11 March 2010
Published 20 April 2010
Online at stacks.iop.org/JPhysCM/22/185802

Abstract

We study triplet migration properties in NPB (N,N'-diphenyl-N,N'-bis(1-naphthyl)-1,1′-biphenyl-4,4″-diamine) films using time resolved gated spectroscopy and dispersive migration theory as our main tools of analysis. We show that in NPB, a well-known hole transporter in organic light emitting diodes, at high excitation densities triplet migration follows two regimes—a dispersive non-equilibrium regime (distinguished by exciton energetical relaxation within the distribution of hopping sites and as a consequence the hopping frequency being time dependent) that evolves into a second, non-dispersive equilibrium regime. Further, we observe a third region, which we term acceleration. From the turning over time between dispersive and non-dispersive dynamics, we deduce the width of the triplet density of states (DOS). We observe how the DOS variance changes when one decreases the thickness of the NPB film and note how surface effects are becoming important. Furthermore, the DOS variance of NPB changes when another organic layer is evaporated on top, namely Ir(piq)3 (tris(1-phenylisoquinoline)iridium(III)). We believe that these changes are due to the different polarizable media in contact with the NPB film, either vacuum or Ir(piq)3. We also show in this paper that the triplet level when time approaches zero is much higher in energy than the relaxed triplet levels, as quoted in most published papers; these values are thus incorrect for NPB. Lastly, it is possible that even at room temperature, the dispersive regime might be important for triplet migration at high initial triplet concentrations and might affect the diffusion length of triplets to a certain extent. However, more experimentation needs to be performed in order to address this question. Overall, we have characterized the triplet migration dynamics of NPB fully and shown that it agrees with previously published observations for other organic semiconductors and theoretical considerations.

(Some figures in this article are in colour only in the electronic version)

1. Introduction

Recently, considerable effort has been put into the research of phosphorescence organic light emitting diodes (PHOLEDs) [1–3]. They are different from conventional fluorescence based OLEDs in that they make efficient use of triplet excitons, which account for 75% of all electron–hole pair recombination events [2]. The most efficient way to do this is to use heavy metal ligand complexes, where triplet emission is enhanced due to spin–orbit coupling. These are doped into a host organic material as emitting species [2] in the emissive layer. However, in order to efficiently transfer triplets from the host material to the dopant, one needs to understand triplet dynamics in the host very well. Furthermore, there is growing evidence that for fluorescent devices triplet–triplet annihilation (TTA) yields extra emission via delayed fluorescence thus improving

[3] Author to whom any correspondence should be addressed.

fluorescence quantum efficiency [4–6]. Some effort has already been put into elucidating the triplet and TTA properties of conjugated polymers [7, 8] and small organic molecules [5, 9, 10]. In addition, Kalinowski *et al* showed that TTA plays a major role in the decrease of the quantum efficiency of electrophosphorescence in OLEDs [11]. However, even for such archetypal transporters as NPB (N,N'-diphenyl-N,N'-bis(1-naphthyl)-1,1′-biphenyl-4,4″-diamine), CBP (4,4-N,N'-dicarbazolyl-1,1′-biphenyl) or TPD (N,N'-diphenyl-N,N'-bis(3-methylphenyl)-[1,1′-biphenyl]-4,4′-diamine) extensively used in PHOLEDs there is very little known [12–14]. The morphological disorder present in these types of materials gives rise to both energetic and positional site distributions, that give rise to dispersive transport and as a consequence, should give a time-dependent triplet diffusion coefficient, which makes analytical treatment very complex [15–18].

Giebink *et al* [14] used time resolved spectroscopy to study triplet diffusion in CBP however there were no experimental results presented on the disorder of the system and the authors used the assumption that triplet migration is non-dispersive at higher temperatures. Indeed, there is no evidence presented throughout their publication showing the presence of a dispersive regime of triplet migration at room temperature. However, Baldo *et al* [13] found evidence that triplet migration in tris(8-hydroxyquinoline) aluminum (Alq3) has a dispersive nature even at room temperature; unfortunately, no detailed account on the dispersive triplet migration can be found in this publication. Thus, it turns out that dispersive transport is relevant in certain OLED materials at room temperature, while in others the impact of it is negligible. Consequentially it is important to gain some insight into fundamental properties of both transport regimes—dispersive and non-dispersive, when and at what temperature the change between the two takes place, how the density of states changes throughout the triplet migration and what is the overall mechanism of TTA. As well, one might question whether there are any changes if one decreases the thickness of film. Although it is possible to study triplet migration and TTA '*in vivo*'—in PHOLEDs— [5], diligent time resolved studies of long lived excited states are very difficult to perform owing to a high RC time constant and other processes such as charge carrier transport. For this reason, we chose to adopt time resolved photoluminescence studies to gain some insight into interesting physical properties of triplet dynamics; both delayed fluorescence and phosphorescence are used to probe triplet movement in the material. We chose NPB as the model material for this research due to its chemical stability, and consequently its consistent photophysical properties, in contrast to some other well-known hole transporters, such as CBP [19].

2. Experimental details

All samples were thermally evaporated using a commercial Kurt Lesker Spectros II deposition system consisting of a vacuum (down to 1×10^{-7} mbar) chamber, six low temperature organic evaporation sources, three metal evaporation sources, quartz sensors to measure the deposition rate and thickness of evaporation, substrate holder, which is normally rotated during the evaporation. All processes are controlled via special software enabling complex OLED device fabrication by sequentially depositing up to six different organic layers as well as metallic cathode without breaking the vacuum. NPB was received from our industrial partner and used without further purification. Thin films were evaporated using the rate of 2 Å s^{-1}, which was much higher than the 0.167 Å s^{-1} evaporation rate previously reported to yield films with high excimer emission [20]. All samples were measured just after evaporation in a vacuum below 1×10^{-4} mbar. Sapphire substrates of 12 mm diameter have been used. Gated luminescence and lifetime measurements were made using a system consisting of excitation source, pulsed YAG laser emitting at 355 nm (EKSMA and CryLas GmbH). Samples were excited at a 45° angle to the substrate plane and the energy of each pulse could be tuned from μJ up to mJ. Emission was focused onto a spectrograph and detected on a sensitive gated iCCD camera (Stanford Computer Optics) with sub nanosecond resolution. Decay measurements were performed by logarithmically increasing gate and delay times; more details can be found elsewhere [7]. For low temperature measurements (down to 12 K) samples were placed in a cryostat.

3. Theoretical framework

One can decompose triplet migration in organic disordered materials into an array of incoherent jumps between the localized energy states, which constitutes the density of states (DOS). It was proven by experiments that after photoexcitation, triplet excitons migrate towards the lower energy tail of the (Gaussian) DOS, thus giving a time-dependent dispersion parameter which complicates the determination of the dynamics of triplets even more [7–10, 15–18]. The exciton behavior in less disordered materials, crystals, has been very well documented by Pope *et al* [21]. There were also some efforts to theoretically describe the migration of excited states in disordered materials [15–18, 22]. Monte Carlo (MC) simulations [23–25] and experimental results using polymers [7, 8] and some small organic molecules [7–10, 26] showed that some of the theoretical considerations could be applied to the interpretation of experiments or calculations. Here, we will outline the theory, which we have used for our triplet migration data analysis. The reader is referred to the original papers for a more rigorous approach [15–18, 22].

Incoherent triplet exciton migration in organic materials is governed by Miller–Abraham equations [17],

$$\begin{aligned} \nu_{ij} &= \nu_0 \mathrm{e}^{-2\beta R_{ij}} \mathrm{e}^{-(E_j - E_i)/kT}, \qquad E_i < E_j, \\ \nu_{ij} &= \nu_0 \mathrm{e}^{-2\beta R_{ij}}, \qquad E_i > E_j, \end{aligned} \tag{1}$$

where T is temperature, k is Boltzmann constant, E energy of the localized state, β is inverse localization length, R_{ij} is the separation between two localized states, ν_0 denotes the attempt-to-jump frequency which is in turn inversely

proportional to the dwell time of an exciton t_0 [18]:

$$t_0 = \frac{1}{\nu_0 6 \mathrm{e}^{(-2\beta R_{ij})}}. \tag{2}$$

Energy matching condition neglect for downward jumps may be justified by low temperature studies of organic glasses, which suggest that energy dissipation does not limit the hopping rate [10]. This might be explained by the phonon rich spectrum in amorphous organic materials and strong electron–phonon coupling which facilitates relaxation [23].

As already mentioned the movement of excited states takes place within a DOS which has an assumed Gaussian distribution [27],

$$n(E) = \frac{1}{(2\pi\sigma^2)^{1/2}} \mathrm{e}^{E^2/2\sigma^2}, \tag{3}$$

σ being the variance of the distribution.

After a laser pulse excitation, intersystem crossing from singlet to triplet manifold takes place, the initial population of triplets is equal to $[T_0]$ (initial condition at $t = 0$, $[T] = [T_0]$), which is then depopulated by monomolecular processes i.e. radiative decay at a rate k_r and non-radiative decay rate k_nr as well as by bimolecular processes, for example, via triplet–triplet annihilation (TTA) rate k_tt [21]:

$$\frac{\mathrm{d}[T]}{\mathrm{d}t} = -(k_\mathrm{nr} + k_\mathrm{r})[T] - k_\mathrm{tt}[T]^2, \tag{4}$$

where $[T]$ denotes the triplet concentration function. Typically, the radiative lifetime of triplet excitons in these materials is very long, in the range of hundreds of milliseconds (especially at low temperatures), thus in most cases monomolecular processes can be neglected. Then we can solve for $[T]$ considering k_tt being time independent. We get:

$$[T] = \frac{[T_0]}{(1 + k_\mathrm{tt}[T_0]t)}, \tag{5a}$$

and for k_tt being time-dependent we get

$$[T] = \frac{[T_0]}{1 + [T_0]\int k_\mathrm{tt}(t)\,\mathrm{d}t}. \tag{5b}$$

If we differentiate (5*a*) we will get an expression for the delayed fluorescence signal arising from TTA:

$$\mathrm{DF} \sim \frac{\mathrm{d}[T]}{\mathrm{d}t} = k_\mathrm{tt}[T_0]^2 \frac{1}{(1 + k_\mathrm{tt}[T_0]t)^2} = k_\mathrm{tt}[T]^2. \tag{6}$$

From this, measurement of the time-dependent DF decay signal will yield the diffusion coefficient D (from k_tt) since it can be expressed in this way [28]:

$$k_\mathrm{tt} = 8\pi f R D, \tag{7}$$

where f is the fraction of triplets annihilated by encounter, and R the interaction radius.

However, it is not simple, if there is a time-dependent, dispersive diffusion coefficient, such as in equation (5*b*). Unfortunately, in disordered materials, this is the case. As mentioned above, triplet diffusion consists of two main regimes, at early times triplet excitons relax towards the low-lying energy sites in the Gaussian DOS. This regime is normally referred to as the non-equilibrium dispersive regime marked by a change of diffusion coefficient $D(t)$ in time. Further, it needs to be said that, while in the dispersive non-equilibrium region the quantity $\mathrm{DF} \sim \mathrm{d}[T]/\mathrm{d}t$ follows a power law $t^{-\alpha}$ with an exponent close to -1 (see section 4 as well) [7, 8, 25]. After a certain time, this regime turns to a classical equilibrium non-dispersive regime, where the diffusion coefficient asymptotically approaches the value D_∞. Then the exponent becomes -2, as one intuitively should expect for a bimolecular decay rate equation (4) and its solution (5*a*). The transition time t_s between the two regimes strongly depends upon the available activation energy, and therefore upon temperature, and the expression it follows has been analytically derived using effective medium approximation techniques by Movaghar *et al* [15] and confirmed by the Monte Carlo (MC) calculations of Ries *et al* [23]:

$$t_s(T) = t_0 \mathrm{e}^{(c\sigma/k_\mathrm{b}T)^2}, \tag{8}$$

where σ is Gaussian density of states variance, c is a constant depending on dimensionality (0.67 in the 3D migration case), t_0 is the dwell time (jump time) for triplets if σ is 0 or if T approaches ∞, and k_b is the Boltzmann constant.

At very low temperatures or in materials having high energy disorder described by the disorder parameter $\sigma^* = (\sigma/k_\mathrm{b}T)$ this transition time becomes infinitely long, i.e. the transport is always dispersive non-equilibrium and the diffusion coefficient depends on time. In other words, the triplets are trapped and the relaxation to the tail of DOS (equilibrium) takes an infinitely long time. Unfortunately it is not possible to cast this time-dependent diffusion coefficient into any simple analytical expression and it heavily depends on activation energy available i.e. temperature. There are a few analytical efforts to do this [15–18], however, the form of the density of states (Gaussian) makes this task difficult and most of the solutions are derived using limiting assumptions. For example, Movaghar *et al* [17] succeeded in deriving the diffusion coefficient expression for highly disordered materials, i.e. when $T \to 0$ and the condition $kT < 0.1\sigma$ is satisfied and when time approaches infinity:

$$D(t) \sim \frac{1}{t \ln(\nu_0 t)}. \tag{9}$$

The other parameter of interest for experimentalists is the peak energy of the DOS distribution needed to determine the non-relaxed triplet levels of the material. As was mentioned, the excited energy randomly distributed at first, migrates downwards the DOS energy tail in time thus preventing us from finding the real triplet energy level at near-zero times since in early times it is very hard to record very weak phosphorescence spectra. However, Richert *et al* [18] derived an expression describing how peak energy of triplet DOS (E_p) changes in the long time limit when $T \to 0$, under the condition $kT < 0.1\sigma$:

$$E_\mathrm{p} \sim -\sigma(3\ln(\ln \nu_0 t))^{1/2}. \tag{10}$$

This expression will enable us to find the unrelaxed triplet energy level of NPB, as the triplet levels, which are normally

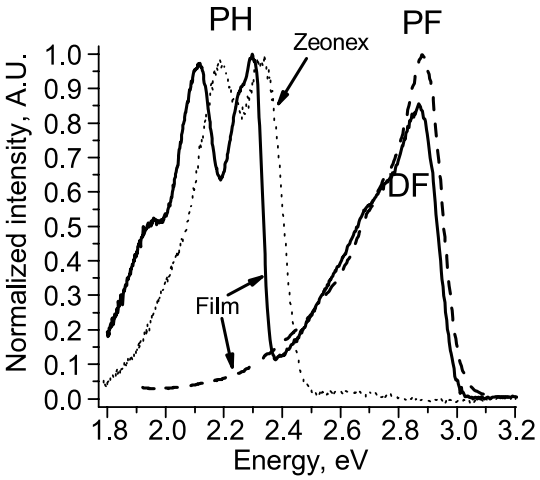

Figure 1. Prompt fluorescence—PF (dashed line), delayed fluorescence—DF (straight line) and phosphorescence—PH (straight line) spectra of evaporated NPB thin film and PH spectrum (dotted line) of NPB in inert Zeonex matrix at dilute concentration (10^{-4} weight to weight ratio). Spectra are normalized to enable comparison since PF intensity has been much higher than DF. PH and DF have been recorded 5 ms after excitation, and PF has been recorded during the first 10 ns after excitation. All spectra recorded at 12 K.

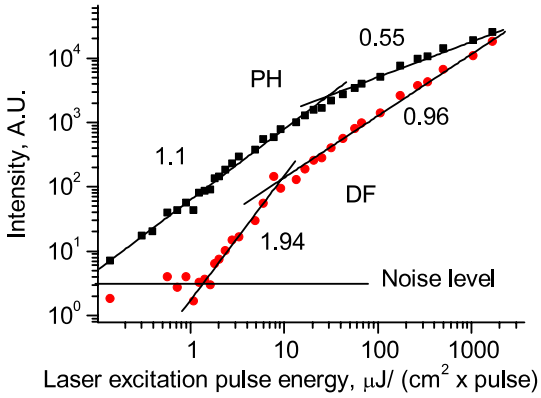

Figure 2. Delayed fluorescence—DF (circles) and phosphorescence—PH (squares) dependence on laser excitation pulse intensity of 250 nm NPB film at 12 K. PH and DF have been recorded 6 ms after excitation, the gate time was 5 ms. Linear curves are fits to PH and DF with the slopes as indicated on the graph. The noise level is indicated as a horizontal dark line in order to show that at very low excitation intensities we do not observe any DF and PH is already present.

measured at very late times after excitation are normally already in the tail of DOS.

4. Results and discussions

Prompt fluorescence (PF), delayed fluorescence (DF) and phosphorescence (PH) spectra of an evaporated NPB thin film are depicted in figure 1. The peak of DF and PF is at ∼2.87 eV and the first vibronic levels of PH are at ∼2.29 eV, which is similar to the literature values [29]. We recorded the PH spectrum of NPB in the inert matrix Zeonex at very dilute concentrations (figure 1), which is blueshifted in comparison with film to ∼2.35 eV. We did not observe any DF from NPB in Zeonex. The PH monoexponential lifetime of NPB in dilute Zeonex was ∼1 s at 14 K indicating very little non-radiative decay in this environment (compare with the film below). Based on the DF and PH dependence on the laser excitation pulse energy we conclude that the DF origin in the films is non-monomolecular (figure 2). Most of the noise in the graph comes from laser shot to shot fluctuations. Initially we observe that PH dependence on excitation intensity has a slope of 1.1 and DF has a slope of 1.94. At higher intensities PH follows the slope of 0.55 and DF follows the slope of 0.96. One would expect to get slopes 1 for PH and 2 for DF assuming that monomolecular decay is dominant, and if bimolecular decay dominates the DF should be proportional to initial excitation and PH intensity should be square root of initial excitation. This is exactly what is observed by us. This type of excitation dose dependence of PH and DF has been already recorded in polyfluorene frozen solutions and films in [7, 8, 30]. Furthermore, the slope of the intensity increase of the DF is twice as large as that of PH, which suggests a bimolecular character of delayed fluorescence emission. In addition to, we can safely reject E-type DF origin, because the difference

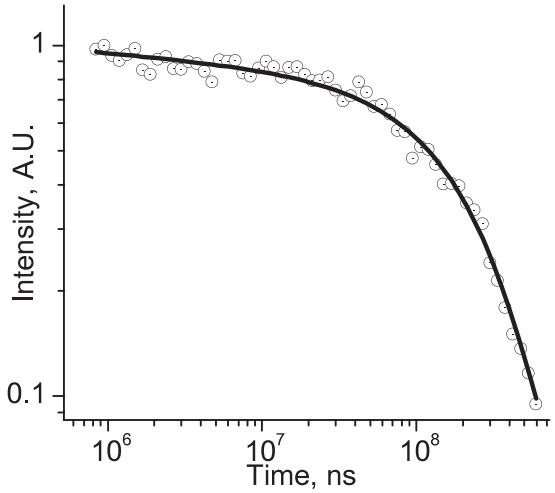

Figure 3. PH decay curve from a 250 nm film at 12 K in a log–log fashion. The black curve corresponds to a fit of the form $t^a \exp(-t/t_1)$ with $a = 0.04$ and $t_1 = 243$ ms. For interpretation, we refer to the text.

between the singlet level and triplet level is 0.55 eV—much more than k_bT at room temperature. So we ascribe DF in NPB to originate from triplet–triplet annihilation (TTA). In all further experiments we used the excitation pulse energy in the region where bimolecular decay is dominant.

In figure 3 the decay curve of the phosphorescence is depicted in a log–log scale. The black curve fitted is proportional to $t^a \exp(-t/t_1)$, with an exponent $a = -0.04$, which is different from the expected value of -1 in equations (5). A similar fit of PH decay of polyfluorene measured using time resolved photoinduced triplet absorption technique has been reported by Rothe *et al* [7] for a polyfluorene derivative. We have chosen the $t^a \exp(-t/t_1)$ function with the value 0.04 instead of the exponential function intentionally. If we assume that triplet concentration in the

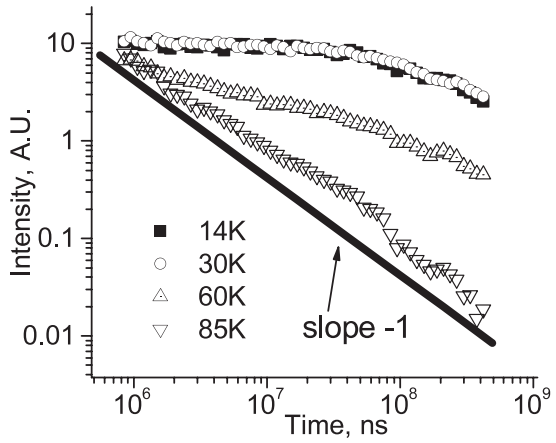

Figure 4. PH decay curves from a 250 nm film at various temperatures in log–log fashion. With an increase of temperature the PH decay approaches t^{-1} i.e. the non-dispersive regime starts to dominate at late times. The straight line is a simulation of how a t^{-1} non-dispersive TTA dominant PH decay would behave.

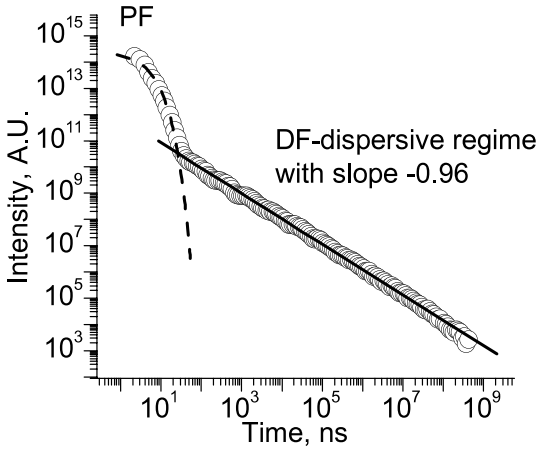

Figure 5. Decay curve of prompt and delayed fluorescence from a 250 nm film at 12 K. The dashed line corresponds to a 3 ns exponential fit of PF; after ∼40 ns the decay starts to follow the power law. This is the decay of DF, with a straight line fit in log–log scale with −0.96 slope.

250 nm film at 14 K decays with $t^{-0.04}$ not t^{-1} and substitute the former value into equation (5*b*) and integrate, we get $k_{tt} \sim t^{-1.04}$. $k_{tt}(t)$ is proportional to $D(t)$ (equation (7)). Then according to equation (9), which has been derived for $T \to 0$, k_{tt} is proportional to $1/[t\ln(\nu_0 t)]$ which in turn can be approximated as $k_{tt}(t) \sim t^{-1.04}$ in the long time limit [24]. Therefore, it would follow that this is not an accidental discrepancy but a clear manifestation of dispersive exciton migration when T approaches 0. We understand that the exponent a is of very small value, making it experimentally very difficult to observe this deviation from pure exponential law, thus we performed more experiments in order to show that the dispersive transport is present in this system.

PH decays versus time on a log–log scale for various temperatures is plotted in figure 4. It is clear that upon increasing the temperature the PH decay approaches a t^{-1} law, i.e. the non-dispersive regime for which equations (5) is valid. These results completely agree with the MC simulations that can be found in [25]. The decays were recorded at late times after excitation, i.e. some 6, 7 orders of magnitude longer and we cannot properly infer from figure 4 how triplets behave at early times. This is in our interest since the migration just after excitation should mainly determine the path length of the triplets' diffusion as well TTA intensity. To gain more insight into triplet migration by using the PH signal is complicated due to DF signal, which is much stronger at early times. In order to understand what is happening just after excitation one needs carefully examine the dynamics of fluorescence states, mainly the dynamics of delayed fluorescence.

The prompt fluorescence lifetime at 12 K of a 250 nm NPB film is 3 ns (figure 5, fitted to dashed line), close to the reported values [31]. However, after ∼40 ns the decay enters a power law regime with a slope of −0.96. For a non-dispersive equilibrium regime where TTA is dominant one should expect the slope of −2 (equations (5*a*) and (6)) which is not the case. Similarly as for PH decay, we can derive the DF decay slope for a TTA dominated dispersive regime. According to equation (9) for highly disordered materials when $T \to 0$, $D(t)$ is proportional to $1/[t\ln(\nu_0 t)]$ [17]. This in turn can be approximated as $D(t) \sim t^{-1.04}$ in the long time limit [24] and $k_{tt}(t) \sim D(t)$. If as shown above triplet concentration decays as $t^{-0.04}$ and we plug the exponents −1.04 and −0.04 into equation (6) we get that DF decays as $t^{-1.12}$ which is close to our value of −0.96. Scheidler *et al* using Monte Carlo simulations [25] have shown that in dispersive triplet migration region PH should decay with power law having slope ∼−0.04 and DF should decay with power low having slope ∼−1. PH decay slope approached −1 and DF decay slope approaches −2 in non-dispersive regime that can easily be derived from equations (5) and (6). In addition to, similar slopes (PH ∼ −0.04 and ∼DF − 1) in the dispersive regime have been observed for conjugated polymers [7, 8]. Thus resting upon theoretical evidence as well as Monte Carlo simulation and similar experimental observations, we ascribe TTA arising from dispersive migration being responsible for the power law with ∼−1 slope regime (figure 5). The discrepancy between the expected (−1.12) and recorded (−0.96) slope values might arise from trap states outside DOS present in film as was suggested in [7]. The triplet trapping rate is hopping limited thus should have the same time dependence as the annihilation rate [9]. This means that triplet trapping and TTA could balance in time giving the similar power law time dependence however with slightly different slope. We would like to point out that the curves, which have been recorded (see e.g. figure 4 85 K curve or figure 5), were due to inherent mobile NPB triplets in NPB density of states. Firstly, as we used gated iCCD we can be sure that the fluorescence spectra recorded at all times were intrinsic to NPB (peak at ∼427 nm compare for example with [20]). In addition, the PH spectra were intrinsic to NPB mobile triplets in NPB DOS peaking at ∼2.31 eV (see e.g. [29]). We did not observe any excimer emission or any aggregate type emission in NPB as in [20]. One would not expect to observe energy relaxation (see below, figure 11) from traps outside the density of states and the power law decays

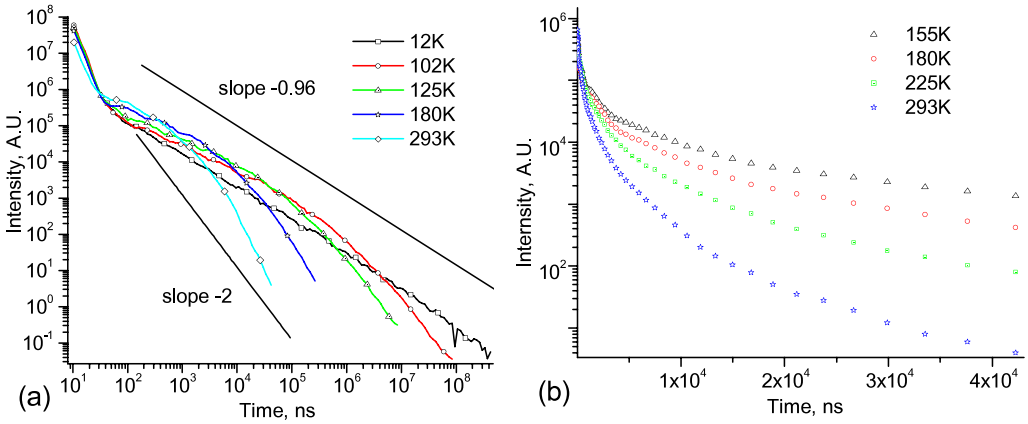

Figure 6. (a) Decay curves from a 250 nm NPB film at various temperatures in a log–log scale. (b) Decay curves at higher temperature in a log–lin scale included with intent to show that the decays are far from exponential. Curves are not normalized.

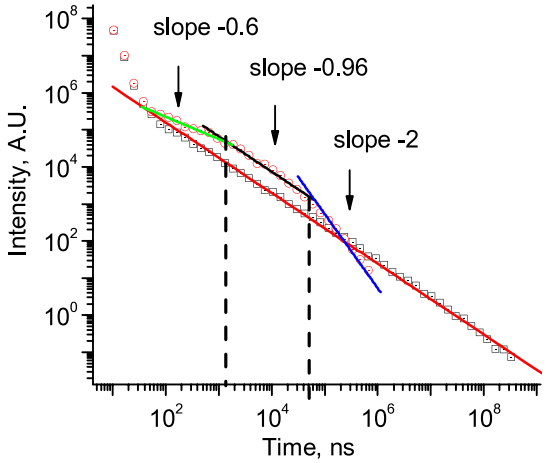

Figure 7. An example of three triplet migration regimes for a TTA curve at 140 K (circles) and their transition time indicated by dashed lines. Squares correspond to a TTA decay at 12 K included for comparison.

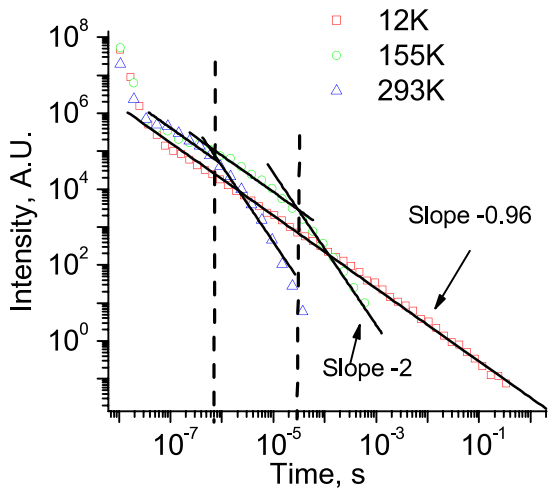

Figure 8. Example of how transition times t_s were determined by using intersections of -0.96 and -2 curves. A linear fit with the slopes of -0.9 and -2 are shown as straight lines and indicated on the graph appropriately. Dashed lines denote the time value of intersection.

from aggregates or traps outside DOS. These decays should be of exponential form (mono, bi, or triexponential etc).

In figure 6, delayed fluorescence decay curves at various temperatures are depicted in a non-normalized fashion. Each curve has been recorded with the same set of parameters enabling intensity comparison. It is clear from the graph that with increasing temperature the DF decay starts to divert from -0.96 slope and approaches classical -2 slope of a non-dispersive equilibrium triplet migration regime. The time at which the transition from the dispersive to the classical non-dispersive regime takes place is called the transition time t_s. In addition to this, around 100–800 ns with an increase of temperature one can observe a gradual increase of DF intensity of slope ~ -0.6 (in figure 7, 140 K decay curve). As can be inferred from figure 6 the same can be easily observed for the decays at higher temperatures up to room temperature. This might be an acceleration region as at higher temperatures more and more triplets can overcome barriers between different energy sites in the DOS. This increase of DF at early times already has been mentioned in some reports with MC calculations of exciton hopping as well been observed in polyfluorene [7, 25, 32]. However, in polyfluorene early delayed fluorescence increases up to 130 K and then decreases after this temperature indicating that some other triplet deactivation process apart from TTA is turned on with an increase in temperature [32]. This means that one could not make use of polyfluorene TTA in organic light emitting devices to extract light as has been done by Kodakov *et al* or Murano *et al* [4–6]. However, NPB would probably be a more suitable candidate for use in OLEDs, where TTA is used to extract additional light as it has a very efficient acceleration region up to room temperature.

An example of how the transition times t_s can be determined is shown in figure 8. The dispersive regime slope has been determined by fitting a 12 K temperature decay curve, that in this case is -0.96. At higher temperature, in this case at 155 K, curves tend to enter the -2 slope regime and the exact time is found by the intersection of -2 and -0.96

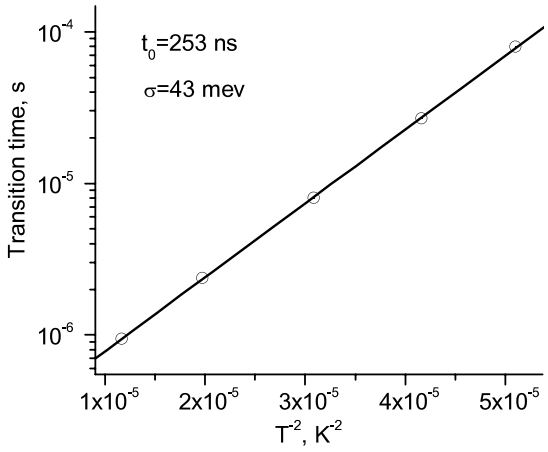

Figure 9. Transition times t_s plotted in semi-logarithmical fashion versus inverse squared temperature.

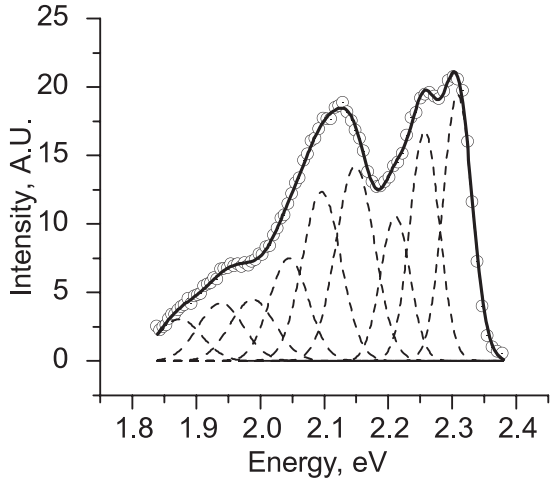

Figure 10. Phosphorescence spectrum of 250 nm NPB film recorded at least 100 ms after excitation at 12 K (black circles). The straight line represents a nine peak Gaussian fit, whereas dashed lines are nine Gaussians fitted. Gaussian variance of the first vibronic band is 45 meV. For the process of fitting we refer to the text.

slope curves (dashed line). The same is done for the 293 K curve. The transition time can be plotted versus the inverse square of temperature, as shown in figure 9. One can fit a linear line in a semi-ln scale and determine the lowest triplet exciton level DOS width, σ, according to equation (8), which for a 250 nm film is equal to 42.9 meV. This value is very similar to values found for polyfluorene by Hertel *et al* [8] (36 meV) and by Rothe *et al* [7] (41 meV). For benzophenone this value was found to be 45.88 meV [10]. Therefore, our value of 43 meV is in the same range as already known experimentally determined DOS variances for other organic disordered materials. Further it is interesting to note that kT at room temperature is ∼25 meV which is almost half the DOS width. Thus, it suggests that even at room temperature we may observe some relaxation towards the edge of DOS i.e. at the beginning the transport will not be in equilibrium. In our opinion, the assumption that only the non-dispersive regime is important at room temperature for all materials at all thicknesses, though in some cases might be valid, should be reconsidered.

The intercept of the curve in figure 10 corresponds to a dwell time t_0 and in our case it is 253 ns. t_0 values of 70 ns and 55 ps for polyfluorene derivatives have been reported in [7] and [8], respectively. Both authors used equation (8) to analyze their data. However, the value of 55 ps was reported for the polyfluorene in frozen methyl tetrahydrofuran (MTHF) matrix between temperatures 100 and 130 K. At these temperatures MTHF does not form a good glass, and it may crystallize, so it is reasonable that TTA has been accelerated by the solvent matrix [7].

Here a word needs to be said about the fitting of DF decay in a non-dispersive regime. We fitted equations (5), which is a simplified solution of equation (4). One could however use the full solution of equation (4) including monomolecular decay to fit instead [33]:

$$[T] = \frac{k_r + k_{nr}}{(k/[T_0] + k_{tt})e^{(k_r+k_{nr})t} - k_{tt}}. \qquad (11)$$

Assuming that the PH intensity is proportion to the triplet concentration $[T]$ and that DF is proportional to $[T]^2$ one could fit squared equation (11) to the non-dispersive decays of DF in order to determine the turnover time between dispersive and non-dispersive regime. Unfortunately we could not simultaneously fit the squared of equation (11) at both dispersive and non-dispersive regions of the DF decay curves (or the fit is not physically meaningful with $k_r + k_{nr} < 0$). In the non-dispersive regions at lower temperatures (of DF decay) the squared equation (11) does not fit as well as equations (5) and this probably reflects the fact that the monomolecular decay rate is very small at low temperatures. At higher temperatures especially at 293 K we could fit equation (11) meaningfully and determine $k_r + k_{nr}$ and k_{tt}, but only to the non-dispersive region of the curve. However, the transition times between dispersive and non-dispersive transition regimes at higher temperatures are similar irrespectively whether one fits equations (11) or (5) to the non-dispersive decay part of curves. Thus for the purpose of determining transitions times equation (11) is not more suitable than equations (5). Furthermore, in [7, 8] authors used equations (5) instead of full solution to determine transition times in conjugated polymers and these systems are very similar to NPB—monomolecular decay of PH at low temperatures in the range of hundreds of milliseconds, triplet DOS in the range of 40 meV.

Another way to find the DOS variance and double check the results would be to fit a Gaussian of the form of equation (2) to the first vibronic levels of the phosphorescence spectrum. In the spectrum one can resolve three broad bands whereas in the first band two vibronic peaks can be seen. Since the first probable vibronic peak of the PH spectrum of NPB overlaps with the second, we fitted totally nine Gaussian peaks with similar width to the PH spectra recorded at 12 K (figure 10). We based our fitting on the infrared and Raman spectra of NPB that can be found in [34, 35]. If we assign the first peak at 2.308 eV (dashed line in figure 10) to the 0–0 vibronic band, the successive eight vibronic bands are approximately 0.051 eV apart from each other. Indeed, there is an intense

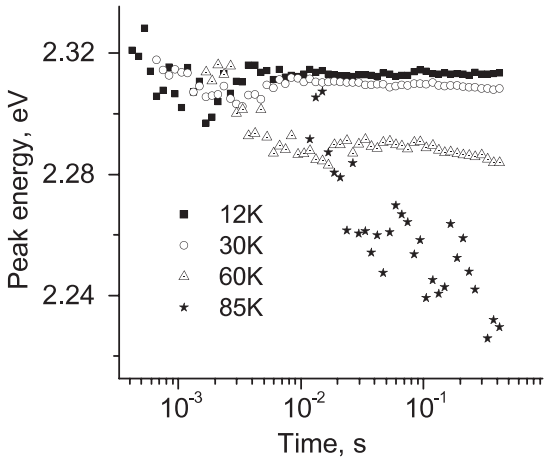

Figure 11. PH first vibronic peak change in time for 250 nm NPB film, at different temperatures. The peak determined by Gaussians fittings to PH spectra.

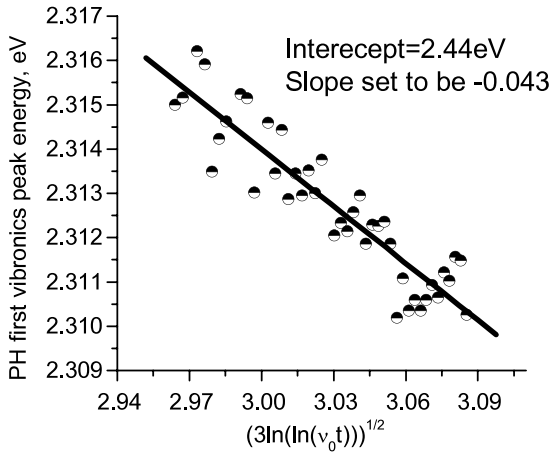

Figure 12. First vibronic peak of PH spectrum at 12 K plotted versus a ln ln timescale. The straight line is a linear fit to the data, slope set to be −0.043, intersecting ordinate axis at 2.44 eV.

peak in infrared spectrum around this energy [35] that has been assigned to CC torsion of naphthyl [34]. Also, referring to the same IR spectra we think, that every second peak (∼0.096 eV apart) could be the CH wag of a naphthyl moiety. Both of those modes are ascribed to the out of plane rotations. Every third peak is 0.16 eV apart and in the IR spectrum [34] as well as in the Raman spectrum [35] this peak is clearly present. In both references it is assigned to CH bend and CN stretch and CCN bend of phenyl. These correspond to in-plane vibrations and are therefore more energetic. Clearly, they constitute a fingerprint of three broad bands we see in figure 10. All of these vibronic modes happened to be multiplies of around 0.05 eV and they are almost superimposed on one another, and thereby broadening the three bands even more as they successively overlap with each other. Thus, they are better resolved only in the first band. It is intuitive to claim that triplet states are localized around nitrogen atom and indeed the assignments we made above only support this, since all in-plane and out-of-plane vibrations and rotations are related to the near proximity of a nitrogen atom, i.e. naphthyl moiety or nitrogen atom itself. The resultant width of the first vibronic band is ∼45 meV, which is in agreement with $\sigma \sim 43$ meV.

In addition, we have observed a freezing-in effect of PH peak energy, which is another manifestation of the non-equilibrium effect in highly disordered materials (figure 11 and see e.g. [18] or [7]). The higher the disorder parameter (the lower the temperature) the longer the time it takes for the relaxation of triplet energy. For a temperature of 12 K, the peak energy of PH relaxes to 2.31 eV only in the first 100 ms, while for 85 K in the same time it relaxes up to ∼2.22 eV. This clearly shows the quasi detrapping of triplets at higher temperatures due to thermally activated hopping thus enabling them to relax earlier and consequently we should expect to see the transition time from dispersive to non-dispersive regime take place earlier for higher temperature decays.

When T approaches 0, the PH peak energy change should follow equation (10). In this way it is possible to find the peak of the first PH vibronic band at time = 0 (i.e. triplet level at time = 0). In figure 12, the peak energy of the PH spectra of a 250 m NPB film at 12 as a function of time on a ln ln scale is depicted ($k_bT/\sigma = 0.02 < 0.1$ for this temperature is much smaller than required so we can apply equation (10) safely). We chose ν_0 to be such that the slope would fit to −0.043 eV and then calculated the ordinate intercept, which we find to be 2.44 eV. This value is much higher than the triplet value for NPB (2.28 eV) published elsewhere [29], and that determined above (∼2.3 eV) by ourselves from phosphorescence spectra. Similar discrepancies have been observed for polyfluorene triplet level [7]. But the higher triplet energy for polyfluorene at time zero determined similarly by authors of [7] agrees well with what has been determined experimentally by pulse radiolysis energy transfer measurements which yields the equivalent $t = 0$ unrelaxed triplet energy [7, 36]. Thus it is probable, that the determined triplet levels E_T (which are normally detected from a phosphorescence spectrum at later times) for other disordered materials, small molecular glasses or conjugated polymer [13, 29], are lower than at time = 0, E_{T0}. Indeed, it is highly possible since normally phosphorescence spectra by most groups are recorded in long time limit when up to 5–6 decades of time have lapsed. This allows triplet excitons to relax to the energy tail of the DOS and thus most of the triplet levels E_T might be lowered in comparison to their true value E_{T0}. We would like to stress that for energy transfer the key value is E_{T0} not E_T.

The same set of experiments has also been repeated for different thickness of NPB films, an example of DF decay curves for 155 K is shown in figure 13. The thinner the film, the faster the dispersive regime changes to a non-dispersive classical triplet migration regime; 13 nm film having the fastest transition time. One should expect a change of t_0 and probably σ with the change of thickness. It is seen from figure 13 and table 1 that this is the case. The thinner the film, the smaller the slope and intercept (exciton dwell time) in the semi-log graph of t_s indicating that with the decrease of thickness, surface effects (surface states) tend to become more important to triplet dynamics. First, surface effects clearly have a huge effect on the dwell time by decreasing it from 257 ns for a 250 nm film

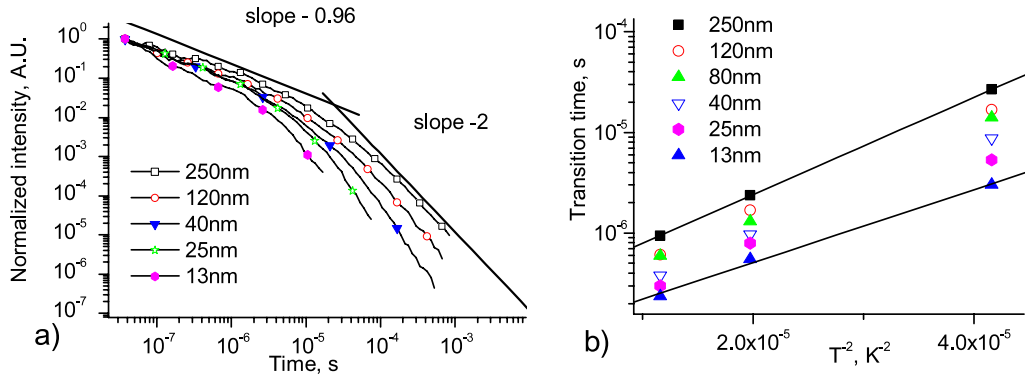

Figure 13. (a) DF decay of NPB at 155 K for various thickness films in log–log scale. Straight lines correspond to linear fits with the slopes −0.96 and −2. (b) Transition times t_s plotted in semi-logarithmical fashion versus inverse squared temperature for NPB films having different thicknesses. The results of linear fits (intercepts and density of state variance) at each thickness are in table 1. Straight black lines are drawn for visualization of different slopes.

Table 1. Intercept, t_0 and slope (density of states variance σ) for NPB films having different thicknesses.

Thickness (nm)	Intercept (ns)	Slope, σ
250	257	42.92
120	177	42.58
80	165	41.89
40	118	41.37
30	114	40.04
25	108	39.48
13	95	37.14

(table 1) to the value of 95 ns for a 13 nm film, which is already close to polyfluorene value of 70 ns [7].

The DOS variance decreases with the decrease of thickness by approximately 13% if one goes from a 250 nm film to a 13 nm film (figure 14). If one plots DOS variance against thickness of film one gets a 1/thickness dependence, with the DOS variance saturating after a certain thickness, indicating that surface states no longer affect the TTA decay, and as a consequence DOS calculations. The DOS width approaches the asymptotic value of 43.07 meV (figure 14). However, for thinner films surface effects might have some significance by decreasing this value. We think this could be the consequence of a Gaussian distribution of energies of excited states. The reason for this type of distribution in organic crystals and glasses is statistical local fluctuations of the polarization energy of a charge carrier and/or the van der Waals energy of excitons [27]. The polarization energy of charge or van der Waals energy of excitons near the surface is clearly different from the polarization energies in the bulk, since near to the surface there is an absence of polarizable medium from the vacuum side. The thinner the film, the more the triplet exciton distribution is determined by energies of surface sites, i.e. smaller statistical fluctuations near surface determine the smaller density of states distribution. As well, it is possible that the bulk morphology is changing with the change of thickness. These might not be the only reasons of a change of the DOS width with the change of thickness. Another reason could be simply the decrease of the number of possible states with the decrease of one of the dimensions

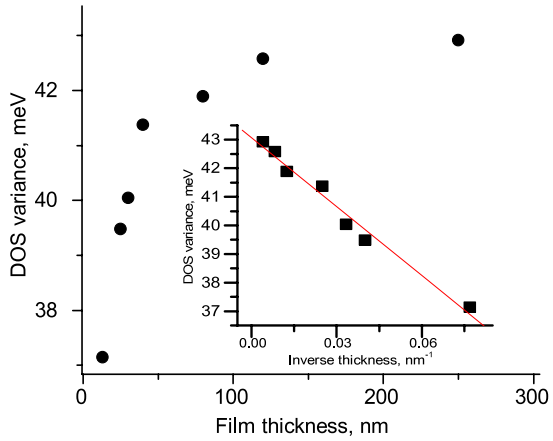

Figure 14. Triplet DOS variance plotted against thickness of NPB film. The resultant curve follows reciprocal function law and approaches asymptotic value of 43.07 meV. Inset: the linear fit of the DOS variance versus inverse thickness.

(thickness). Although it is very difficult to quantify it, if one decreases the volume by sufficient amount it is possible that the DOS decreases by the virtue of the decrease of number of possible excitonic states. Although this seems a plausible reason for a decrease of DOS width, we prefer the former explanation; further experiments described below supply more evidence towards the first hypothesis of surface state effects.

Repeating the experiments described above for NPB films with a 33 nm Ir(piq)3 film on top of each NPB film we observe a different dependence of DOS width with the decrease of thickness of NPB film. It does not look at first sight that the dependence follows the reciprocal law (figure 15), and it looks like the DOS saturates as the film gets thinner. However, we note that it might follow a 1/thickness law for even thinner films (<13 nm), the decay curves of which are quite difficult to record due to the weak signal. These results show that an Ir(piq)3 film, instead of vacuum, changes the local statistical fluctuations of surface states (as well as DOS distribution). This is another reason why we think that the main reason for a change in DOS with thickness is the surface state effect rather

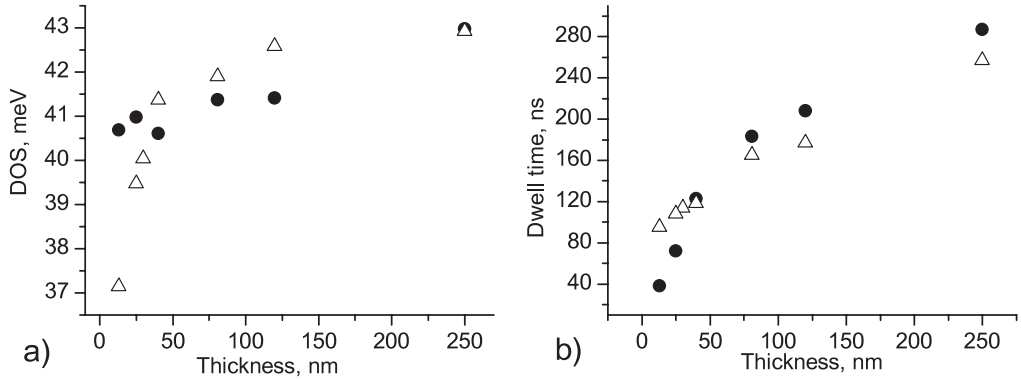

Figure 15. Triplet DOS variance (a) and dwell time (b) plotted against thickness of NPB film in NPB/Ir(piq)3 bilayer film (black circles). The NPB/Ir(piq)3 was excited from NPB side and Irpiq thickness in bilayer all the time was 33 nm. For comparison the DOS variance of NPB film only is plotted as triangles.

than the decrease of total possible density of states as discussed above. Of course this is not conclusive evidence as it has been done only with one material, and further experimental evidence needs to be collected, for example, using other materials, but the change of DOS width when another material is on top of NPB nicely fits with surface state effect hypothesis.

Further, we would like to draw the reader's attention to the very important application consequence of this dependence on the DOS. If one puts another layer instead of NPB on top, for example CBP, one might expect a different DOS variance change with thickness due to the different polarizability properties of a CBP film and as a consequence the same thickness NPB films might have a different DOS width.

The dwell time dependence on thickness changes after the addition of the Irpiq layer, as well (figure 15). For very thick films above 100 nm the Ir(piq)3 layer increases the dwell time whereas for thinner films, especially below 50 nm, the dwell time is significantly decreased for an NPB/Ir(piq)3 film complex in comparison with an NPB/vacuum film. This decreased dwell time shows that there is movement or diffusion of triplets from NPB film to the Ir(piq)3 film (publication is in preparation).

5. Conclusions

Triplet migration properties of NPB thin films have been reported. The phosphorescence lifetime at 12 K was determined to not follow an exponential decay law but a $t^a \exp(-t/t_1)$ law with an exponent a equal to -0.04. Intensity dependencies of PH and DF suggest that DF in NPB films is from triplet–triplet annihilation (TTA). The triplets of NPB films decay in a similar fashion to that which has been predicted theoretically, as well as by MC simulations and it follows the same pattern as was determined experimentally for conjugated polymers. At first, the dispersive non-equilibrium regime with the slope -0.96 prevails, whereas later it turns to a classical -2 slope for a non-dispersive equilibrium regime. From the turning points between the two regimes at various temperatures, we have determined the variance of Gaussian triplet density of states for various thicknesses films. It approaches an asymptotic value of 43.07 meV for infinite thickness, which we think, is the real DOS variance for an NPB film in which surface states do not have any importance. However, for thinner films, for example, of 13 nm, the DOS variance decreases to ∼37.14 meV. If one puts an Ir(piq)3 film on top, then the DOS does not decrease so significantly as for the NPB film on its own, indicating that a polarizable medium near the NPB surface has an impact for NPB DOS variance. Furthermore, we believe that our results demonstrated that for high excitation doses even at room temperature the dispersive regime is still present for some time. The question whether it has a large influence to the pathlength of migrating excitons in organic film remains unanswered and more experiments need to be done to address this question. Finally, we determined the unrelaxed triplet level of the NPB thin film at zero time (the peak of the first vibronic band of PH spectrum), which is 2.44 eV—slightly higher than was determined from late gated phosphorescence spectra, but must be considered when describing energy transfer processes between NPB and dopant.

Acknowledgments

The authors thank the Eastman Kodak Company for the materials, and also Kodak European Research for the studentship for VJ.

References

[1] D'Andrade B W, Brooks J, Adamovich V, Thompson M E and Forrest S R 2002 *Adv. Mater.* **14** 1032–6
[2] Sun Y, Giebink N C, Kanno H, Ma B, Thompson M E and Forrest S R 2006 *Nature* **44** 908–12
[3] D'Andrade B W, Forrest S R and Chwang A B 2003 *Appl. Phys. Lett.* **83** 3858
[4] Murano S, He G, Pavicic D, Denker U, Rothe C, Hofmann M, Werner A and Birnstock J 2008 *The 7th Int. Conf. on Electroluminescence of Molecular Materials and Related Phenomena, Invited Lecture 10* (from Novaled AG)
[5] Kondakov D Y 2007 *J. Appl. Phys.* **102** 114504
[6] Kondakov D Y 2009 *J. Soc. Inform. Display* **17** 137–44
[7] Rothe C and Monkman A P 2003 *Phys. Rev.* B **68** 075208
[8] Hertel D, Bassler H, Guentner R and Scherf U 2001 *J. Chem. Phys.* **115** 21
[9] Lange J, Ries B and Bassler H 1988 *Chem. Phys.* **128** 47–8
[10] Richert R and Bassler H 1986 *J. Chem. Phys.* **84** 6

[11] Kalinowski J, Stampor W, Mezyk J, Cocchi M, Virgili D, Fattori V and Di Marco P 2002 *Phys. Rev.* B **66** 235321
[12] Reineke S, Walzer K and Leo K 2007 *Phys. Rev.* B **75** 125328
[13] Baldo M A and Forrest S R 2000 *Phys. Rev.* B **62** 10958–66
[14] Giebink N C, Sun Y and Forrest S R 2006 *Org. Electron.* **7** 375–86
[15] Grunewald M, Pohlmann B, Movaghar B and Wurtz D 1984 *Phil. Mag.* B **49** 341–56
[16] Movaghar B, Grunewald M, Ries B, Bassler H and Wurtz D 1986 *Phys. Rev.* B **33** 5545–54
[17] Movaghar B, Ries B and Grunewald M 1986 *Phys. Rev.* B **34** 5574–82
[18] Richert R, Bassler H, Ries B, Movaghar B and Grunewald M 1989 *Phil. Mag. Lett.* **59** 95–102
[19] Jankus V, Winscom C and Monkman A P 2009 *J. Chem. Phys.* **103** 074501
[20] Losio P A, Khan R U A, Gunter P, Yap B K, Wilson J S and Bradley D D C 2006 *Appl. Phys. Lett.* **89** 041914
[21] Pope M and Swenberg C E 1982 *Electronic Processes in Organic Crystals* (New York: Oxford University Press)
[22] Rudenko A I and Bassler H 1991 *Chem. Phys. Lett.* **182** 6
[23] Ries B, Bassler H, Grunewald M and and Movaghar B 1988 *Phys. Rev.* B **37** 5508–17
[24] Ries B and Bassler H 1987 *J. Mol. Electron.* **3** 15–24
[25] Scheidler M, Cleve B, Bassler H and Thomas P 1994 *Chem. Phys. Lett.* **225** 431–6
[26] Richert R and Bassler H 1985 *Chem. Phys. Lett.* **118** 235–9
[27] Bassler H 1981 *Phys. Status Solidi* b **107** 9–64
[28] von Smoluchowski M 1917 *Z. Phys. Chem. Stoechiom. Verwandschaftsl.* **92** 129
[29] Yersin H (ed) 2008 *Highly Efficient OLEDs with Phosphorescence Materials* (Weinheim: Wiley–VCH)
[30] Rothe C and Monkman A P 2002 *Phys. Rev.* B **65** 073201
[31] Kawamura Y, Yamamoto H, Goushi K, Sasabe H and Adachi C 2004 *Appl. Phys. Lett.* **84** 2724–6
[32] Rothe C, Guentner R, Scherf U and Monkman A P 2001 *J. Chem. Phys.* **115** 9557
[33] Dicker G, de Haas M P and Siebbeles D A 2005 *Phys. Rev.* B **71** 155204
[34] Halls M D, Tripp C P and Bernhard Schlegel H 2001 *Phys. Chem. Chem. Phys.* **3** 2131–6
[35] Sugiyama T, Furukawa Y and Fujimura H 2005 *Chem. Phys. Lett.* **405** 330–3
[36] Monkman A P, Burrows H D, Hartwell L J, Horsburgh L E, Hamblett I and Navaratnam S 2001 *Phys. Rev. Lett.* **86** 1358